ASIAN JOURNAL OF CIVIL ENGINEERING (BHRC) VOL. 16, NO. 4 (2015)
PAGES 467-492

A COMPARATIVE STUDY OF SLOPE STABILITY ANALYSIS USING TRADITIONAL LIMIT EQUILIBRIUM METHOD AND FINITE ELEMENT METHOD

A. Burman[1*], S. P. Acharya[2], R. R. Sahay[3] and D. Maity[4]
[1]Department of Civil Engineering, National Institute of Technology, Patna, India
[2]Birla Institute of Technology, Mesra, Ranchi, India
[3]Department of Civil Engineering, Birla Institute of Technology, Patna, India
[4]Department of Civil Engineering, Indian Institute of Technology, Kharagpur, India

Received:12 October 2014; **Accepted:**2 February 2015

ABSTRACT

Traditional limit-equilibrium techniques are the most commonly-used analysis methods for slope stability problems. Recently, finite element method has emerged as an efficient and viable tool for analyzing various geotechnical problems. The Strength Reduction Technique (SRT) technique enables the FEM to calculate factors of safety for slopes. Despite the SRT's many obvious benefits, it has not yet received widespread acceptability among geotechnical engineers for routine slope stability analysis. To help change this situation this paper will compare the method's performance to those of the most widely used limit-equilibrium methods on a broad range of slope stability problems.

Keywords: Slope stability; limit equilibrium methods; finite element method; strength reduction technique; Bishop's method; Spencer's method; Morgenstern and price's method.

1. INTRODUCTION

The stability of earth embankments or slopes, as they are commonly called, should be very thoroughly analysed since their failure may lead to loss of human life as well as colossal economic loss. The primary purpose of slope analysis in most engineering application is to contribute to the safe and economic design of excavations, embankments, earth dams etc. The failure of a mass of soil located beneath a slope is called a slide. It involves a downward and outward movement of the entire mass of soil that participates in the failure. The failure of slopes takes place due to (i) the action of gravitational forces, and (ii) seepage forces within the soil .They may also fail due to excavation or undercutting of its foot, or due to

*E-mail address of the corresponding author: avijitburman@yahoo.com (A. Burman)

gradual disintegration of the structure of the soil. Slides may occur in almost every conceivable manner, slowly or suddenly, and with or without any apparent provocation.

The economic losses associated with slope movements reach about US$ 4.5 billion per year in Japan, US$ 2.6 billion in Italy, on the order of US$ 2 billion in the United States, and US$ 1.5 billion in India [1]. A further account of 'annual losses from naturally disasters generally, to which landslides contribute significantly, are estimated by the UN Disaster Relief Coordinator to amount to 1 or 2 % of the gross national products in many developing countries' [2]. A dramatic Problem was provided in 1993 by the 'La Josephina' landslide, which created a 90 m high dam with 180-hm^3 reservoir that failed 33 days later. Seventy-one persons died, and the direct cost was US$ 141 million: that is, 1.24% of the gross natural product of Ecuador [1].

Human casualties related to land slides are also important. This can be illustrated by the situation in China, which is probably the country that suffers the most from the facilities due to landslides. It includes the earthquake-induced Haiyuan landslides, which killed 100000 (possibly 200000) people; it also include the Dong Xiang landslides, which in 1983 killed more than 200 people. historical records show that the number of landslides-related fatalities in China exceeds 100 per year [3]. Also, very recently the state of Sikkim in India suffered a major slope failure on 18th September, 2011 due to excessive rainfall which led to the loss of lives, blockage of roads and disruption of public transport system.

Traditional limit-equilibrium techniques are the most commonly-used analysis methods for slope stability problems. They approach the problem with a few assumptions: i) A pre-determined failure mechanism is assumed, ii) Normally the analysis is carried out in a 2-D framework ignoring the 3-D effects (although in reality slopes are three dimensional), iii) The soil mass is assumed to move as a rigid block, with the movement only taking place along the failure surface itself, iv) It is assumed that the mobilisation of shear stresses occurs locally. Normally, the shear stresses are not usually uniformly mobilised over the whole length of the failure surface. However, for the purpose of analysis, we assume they are.

In the assessment of slopes, engineers primarily use factor of safety values to determine how close or far slopes are from failure. The basis for most limit equilibrium methods of slope stability analysis can be traced back to 1922, when the Geotechnical Commission was appointed by the Swedish State Railways to investigate solutions following a costly slope failure. The method has become known has the Swedish Slip Circle Method. This method assumes the slide occurs along a circular arc. Fellenius [4] developed this method further, creating a method known as the "Ordinary Method of Slices" or Fellenius' method. In any method of slices, the soil mass above the failure surface is subdivided into vertical slices, and the stability is calculated for each individual slice. Fellenius' Method simplifies the equation by assuming that the forces acting on the sides of each slice cancel each other. While this enables a solution to be determined, the assumption is not completely correct, and leads to low values for the computed Factor of Safety.

The approach was refined by accounting for the interslice normal forces, thus calculating the factor of safety (FOS) with increased accuracy. The method of slices thus developed is known as the "Simplified Bishop's Method" [5]. However, Bishop's Method still does not satisfy all the conditions of static equilibrium (i.e., summation of horizontal forces is missing); therefore, it is an 'incomplete equilibrium method'.

In 1967, Spencer [6] developed a complete equilibrium method known as Spencer's

Method, which satisfies both force and moment equilibrium forces. As a result, the FOS calculated by this method should be more precise. This method can also be adapted for use with non-circular slip surfaces, which is useful because many slope failures do not have circular failure surfaces.

Other methods of slices for calculating stability for non-circular failure surfaces include "Janbu's Rigorous Method" and "Janbu's Simplified Method" [7]. His rigorous method accounts for the interslice forces; his simplified method assumes these forces are zero, but includes a correction factor to compensate for the interslice forces. An alternative method for analyzing slides with a noncircular failure path was developed by Morgenstern and Price [8]. This method satisfies all equations of statical equilibrium, and is known as the "Morgenstern-Price Method".

The limit equilibrium method of slices is based on purely on the principles of statics; that is, the summation of moments, vertical forces, and horizontal forces. The method says nothing about stress, strain and displacements, and as a result it does not satisfy displacement compatibility. It is the key piece of missing physics that creates many of difficulties with limit equilibrium method. Overcoming the gap left by the missing piece of physics means somehow incorporating a stress-strain constitutive relationship into the formulation. One way of doing this is to use FEM instead of determining the stresses from equation of statics.

Although finite element method (FEM) has been commonly used in deformation analysis of embankments and other geotechnical problems, it is still not widely used for stability analysis of slope as compared to conventional limit equilibrium methods [9, 10]. FEM involves more complex theory and it usually requires more time for developing model parameters, performing the computer analyses and interpreting the results [9]. Despite that, the FEM for slope stability analysis have several advantages over the conventional limit equilibrium methods, as stated by Griffiths and Lane [10]:

1) In this method, no assumptions are needs to be made in advance about the shape or location of failure surface. Failure occurs "naturally" through the zones within the soil mass in which the soil strength is unable to resist the applied shear stresses.

2) Since there is no concept of slices in the finite element approach there is no need for assumptions about slice side forces. The finite element method preserves global equilibrium until "failure" is reached.

3) If realistic soil compressibility data is available, the finite element solutions will give information about deformations at working stress levels.

4) The finite element method is able to monitor progressive failure up to and including overall shear failure.

One of the earliest studies that used the FEM for stability analysis of slopes was Smith and Hobbs [11]. Based on the elasto-plastic soil model, they reported results of $\phi_u = 0$ slopes and obtained reasonable agreement with Taylor's charts [12]. Meanwhile, studies were conducted to analyse the stability of $c' - \phi'$ slopes using the FEM [13, 14]. These studies also indicated that the FOS computed by the FEM was in good agreement with that calculated by limit equilibrium methods. Since then, more studies adopting for slope stability analysis have been reported [10, 15, 16, 17].

This two-dimensional ($2D$) elasto-plastic finite element software was developed and updated to include a better slope geometry routine [18]. It was later extended to three-dimensional ($3D$) analysis [19] in the fourth edition of the text. This finite element slope stability analysis software has been rigorously tested and validated against the limit equilibrium method [10]. They showed that the computer program can be applied to slopes under different conditions including undrained clay ($\phi_u = 0$) slopes, $c' - \phi'$ slopes, layered slopes and slopes with a free surface. Meanwhile, Lane and Griffiths (2000) used the same computer program to estimate the stability of slope under a drawdown condition and comparisons were made with the limit equilibrium results published by Morgenstern [8]. The progression of failure within a slope under different loading strategies using the same computer program was carried out [20]. More recently, studies were conducted using the 3D version of the FEM computer program for the slope stability analysis and made comparisons with other 3 D limit equilibrium methods [21]. The 2D version of the finite element slope stability program has been used throughout this work. The theoretical aspects and formulation of the finite element slope stability model will be discussed in the subsequent part.

Recently, however, the significant computing and memory resources available to the geotechnical engineer, combined with low costs, have made the FEM a powerful, viable alternative. The Strength Reduction Technique (SRT) enables the FEM to calculate factors of safety for slopes [22, 10]. The method enjoys several advantages including the ability to predict stresses and deformations of support elements, such as piles, anchors and geotextiles, at failure. As well the technique makes it possible to visualize the development of failure mechanisms. Despite the SRT finite element technique's many benefits, it has not received widespread acceptance among geotechnical engineers for routine slope stability analysis. In the authors' opinion this is primarily due to the very limited experience engineers have had with the tool for slope stability analysis and the limited published information on the quality/accuracy of its results. To improve confidence in the SRT, this paper will compare the method's performance to those of well-established limit-equilibrium methods on a broad range of slope stability problems.

2. MATHEMATİCAL MODELS

2.1 Slope stability analysis using limit equilibrium method

In the conventional limit equilibrium approach, the stability of a slope measured by *factor of safety* (FOS), which is defined as the ratio between the shear strength of the soil to shear stress required to maintain the equilibrium of the slope [9]. A slip surface, which can be planar, circular or non-circular in shape, is required to be assumed prior to the equilibrium analysis. At that point of failure the shear strength is assumed to be fully mobilized along the slip surface and FOS is assumed to be constant for the entire slip surface. The stability analysis eventually involves an iterative process until the critical slip surface is found out where the critical slip surface is defined as the slip surface with lowest FOS. Over the years, many studies have been conducted to investigate the computational accuracy of different limit equilibrium methods and to develop techniques for searching the critical slip surface [9]. However, he pointed out that the critical slip surface can be assumed to be circle, in

most cases, with little inaccuracy unless there are geological layers that constrain the slip surface to a non-circular shape.

An analysis of slope stability begins with the hypothesis that the stability of a slope is the result of downward or motivating forces (i.e., gravitational) and resisting (or upward) forces. These forces act in equal and opposite directions as can be seen in Fig. 1. The resisting force must be greater than the motivating forces in order for a slope to be stable. The relative stability of a slope (or how stable it is at any given time) is typically conveyed by geotechnical engineers through a Facto of Safety FOS defined as follows:

$$FOS = \frac{\sum R}{\sum M} \tag{1}$$

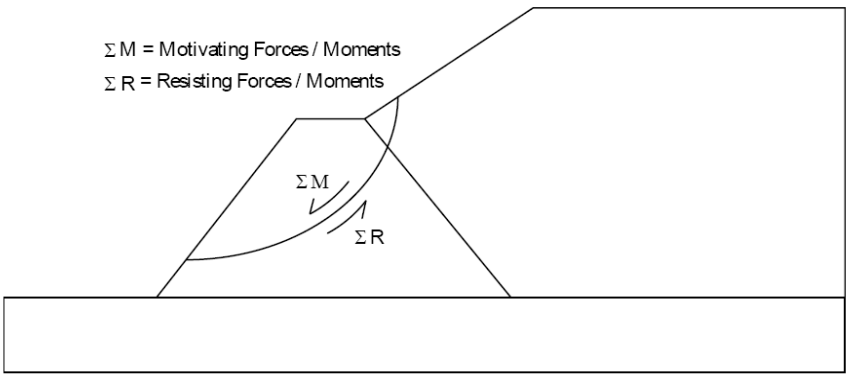

Figure 1. Illustration of the motivating and resisting forces/moments involved in a slope stability analysis

The eq. (1) states that the factor of safety is the ratio between the forces/moments resisting (R) movement and the forces/moments motivating (M) movement. When the factor of safety is equal to 1.0 a slope has just reached failure conditions. If the factor of safety falls below 1.0 then failure is imminent, or has already occurred. Factors of safety in the range of 1.3 to 1.5 are considered reasonably safe in many design scenarios. However, the actual factor of safety used in design is influenced by the risk involved as well as the certainty with which other variables are known.

In the present study, the slice technique is used for slope stability analysis. The forces acting on a typical slice are shown in Fig. 2, where $W =$ weight of slice, $kW =$ seismic force applied to centre of slice, $S/F =$ mobilized shear force at base of a slice, $P' =$ effective normal forces on base , $U =$ water pressure force on base, $B =$ resultant top boundary force, $X =$ vertical side force, $E =$ horizontal slide force. In this work, four different types of limit equilibrium techniques have used. They are: a) Ordinary slice method, b) Bishop's method, c) Spencer's Method and d) Morgenstern and Price method to analyze stability of various types of slopes.

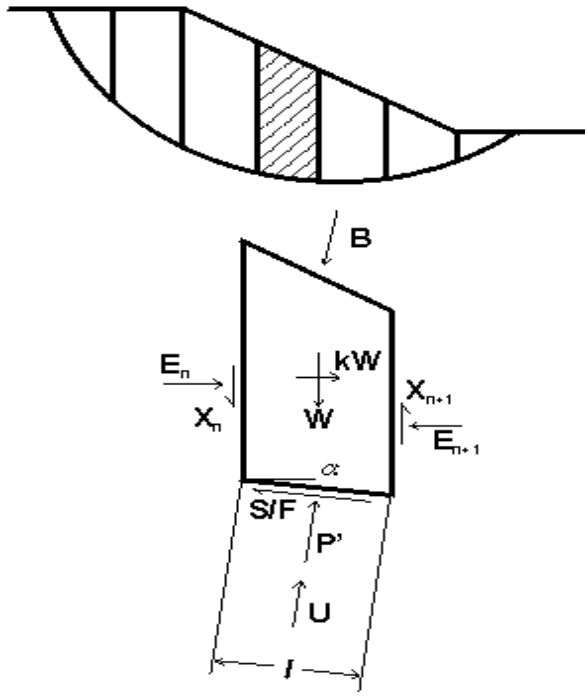

(a) Forces acting on a typical slice

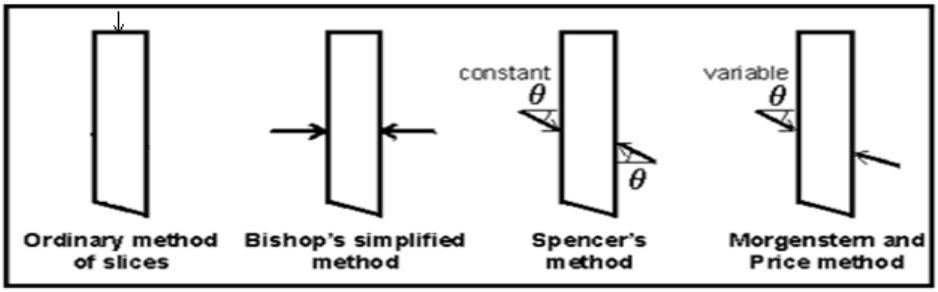

Figure 2. (b) Differences in assumptions regarding side forces in common methods of slope stability analysis

As stated previously, equilibrium methods employ assumptions to make the problem statically determinate. The most critical of these assumptions typically deals with the side forces *X* and *E*. Fig. 2 shows the assumption made concerning side forces for the methods which have been used in this study.

The method proposed by Fellenius [4] is also called "Ordinary Method of Slices". It is applicable only for circular slip surfaces. It satisfies one equation (moment equilibrium of entire mass).

In the 1950's Professor Bishop at Imperial College in London devised a method which included interslice normal forces, but ignored the interslice shear forces. Bishop's method only satisfies moment equilibrium. Including the interslice normal forces means that Bishop's method is close to being in force equilibrium, as indicated by the force polygon for each slice [5]. Bishop developed an equation for the normal at the slice base by summing

slice forces in the vertical direction. The consequence of this is that the base normal becomes a function of factor of safety. This in turn takes factor of safety equation nonlinear (that is, FOS appears on both the sides of the equation) and an iterative procedure is consequently required to compute factor of safety.

Spencer's method satisfies all conditions of equilibrium. It is applicable to any shape of slip surface. It assumes that inclinations of side forces are the same for every slice. Side force inclination is calculated in the process of solution so that all conditions of equilibrium are satisfied. It is an accurate method [6].

Morgenstern and Price's [8] method satisfies all conditions of equilibrium. It is applicable to any shape of slip surface. It assumes that inclinations of side forces follow a prescribed pattern, called f(x). Side force inclinations can be the same or can vary from slice to slice. Side force inclinations are calculated in the process of solution so that all conditions of equilibrium are satisfied. It is an accurate method. The interslice functions available in software SLOPE/W for use with the Morgenstern-Price (M-P) method are: a) Constant, b) Half-sine, c) Trapezoidal and d) Data-point specified. Selecting the Constant function makes the M-P method identical to the Spencer method. But, in this paper half-sine is used for slope stability analysis purpose.

2.2 Slope stability analysis using finite element method

2.2.1 Determination of factor of safety

The Factor of Safety (*FOS*) of a soil slope is defined here as the factor by which the original shear strength parameters must be divided in order to bring the slope to the point of failure. The factored shear strength parameters c'_f and ϕ'_f are therefore given by:

$$C'_f = \frac{C'}{SRF} \tag{2}$$

$$\phi'_f = \tan^{-1}\left(\frac{\tan\phi'}{SRF}\right) \tag{3}$$

Where *SRF* is a “Strength Reduction Factor”. This method is referred to as the “shear strength reduction technique” [23] and allows for the interesting option of applying different strength reduction factors to the c' and $\tan\phi'$ terms. In this paper however, the same factor is always applied to both terms. To find the “true” factor of safety *FOS* ,it is necessary to initiate a systematic search for the value of *SRF* that will just cause the slope to fail. When this value has been found, *FOS* = *SRF*.

According to Smith and Griffith [19], non-convergence within a user-specified number of iteration in finite element program is taken as a suitable indicator of slope failure. This actually means that no stress distribution can be achieved to satisfy both the Mohr-Coulomb criterion and global equilibrium. Slope failure and numerical non-convergence take place at the same time and are joined by an increase in the displacements. Usually, value of the maximum nodal displacement within the mesh just after slope failure has a big jump compared to the one before failure. If the algorithm is unable to satisfy these criteria, “failure” is said to have occurred. Most of the results shown in this work used an iteration

ceiling of 1000 and present results in the form of a graph of SRF vs. $E'\delta_{\max}/\gamma H^2$ (a dimensionless displacement), where $\delta_{\max}$ the maximum nodal displacement at convergence and H is the height of the slope. This graph may be used alongside the displaced mesh and vector plots to indicate both the factor of safety and the nature of the failure mechanism.

2.2.2 Mohr-coulomb failure criteria

In the present work, two-dimensional plain-strain models are used to represent the slope failure problems. The Mohr-Coulomb constitutive model is used to describe the soil (or rock) material properties. The Mohr-Coulomb criterion relates the shear strength of the material to the cohesion, normal stress and angle of internal friction of the material. The failure surface of the Mohr-Coulomb model can be presented as [19]:

$$F = \frac{I_1}{3}\sin\phi + \sqrt{J_2}\left[\cos\theta - \frac{1}{3}\sin\theta\sin\phi\right] - C\cos\phi \tag{4}$$

Where φ is the angle of internal friction, *C* is cohesion and

$$I_1 = (\sigma_1 + \sigma_2 + \sigma_3) = 3\sigma_m \tag{5}$$

$$\theta = \frac{1}{3}\sin^{-1}\left[\frac{3\sqrt{3}J_3}{2J_2^{3/2}}\right] \tag{6}$$

$$J_2 = \left(\frac{1}{2}\left(S_x^2 + S_y^2 + S_z^2\right) + \tau_{xy}^2 + \tau_{yz}^2 + \tau_{zx}^2\right) \tag{7}$$

Where, $J_3 = s_x s_y s_z + 2\tau_{xy}\tau_{yz}\tau_{zx} - s_x\tau_{yz}^2 - s_y\tau_{xz}^2 - s_z\tau_{xy}^2$ (8)

Also, $s_x = \sigma_x - \sigma_m, s_y = \sigma_y - \sigma_m$ and $s_z = \sigma_z - \sigma_m$ (9)

For Mohr-Coulomb material model, six material properties are required. These properties are the friction angle φ, cohesion *C*, dilation angle ψ, Young's modulus *E*, Poisson's ratio ν and unit weight of soil γ. Young's modulus and Poisson's ratio have a profound influence on the computed deformations prior to slope failure, but they have little influence on the predicted factor of safety in slope stability analysis. Dilation angle, ψ affects directly the volume change during soil yielding. If ψ = φ, the plasticity flow rule is known as "associated flow rule", and if ψ ≠ φ, the plasticity flow rule is considered as "non-associated flow rule". The change in the volume during the failure is not considered in this study and therefore the dilation angle is taken as 0. Therefore, only three parameters (friction angle, cohesion and unit weight of material) of the model material are considered in the modelling of slope failure.

2.2.3 Generation of body loads using finite element method

Constant stiffness methods use repeated elastic solutions to achieve convergence by iteratively varying the loads on the system [19]. Within each load increment, the system of equations.

$$[K_m]\{U\}^i = \{F\}^i \tag{10}$$

In this equation, global displacement increments is given by $\{U\}^i$, i represents the iteration number, $[K_m]$ the global stiffness matrix, and $\{F\}^i$ the global external and internal (body) loads. The element displacement increments $\{u\}^i$ are extracted from $\{U\}^i$, and these lead to strain increments via the element strain-displacement relationships:

$$\{\Delta \in\}^i = [B]\{u\}^i \tag{11}$$

Assuming the material is yielding, the strains will contain both elastic and (visco) plastic component, thus

$$\{\Delta \in\}^i = \{\Delta \in^e\}^i + \{\Delta \in^p\}^i \tag{12}$$

It is only the elastic strain increments $\{\Delta \in^e\}^i$ that generates stress through elastic stress-strain matrix, hence

$$\{\Delta\sigma\}^i = [D^e]\{\Delta \in^e\}^i \tag{13}$$

These stresses increment are added to stresses already existing from the previous load step and updated stresses substituted into the failure criterion (4). If stress redistribution is necessary (i.e. the yield function $F > 0$), this is done by altering the load increment vector $\{F\}^i$ in eq. (10). In general, this vector holds two types of load, as given by

$$\{F\}^i = \{F_a\} + \{F_b\}^i \tag{14}$$

where $\{F_a\}$ is actually applied external load increment and $\{F_b\}^i$ is the body loads vector that varies from one iteration to next. The $\{F_b\}^i$ vector must be self-equilibrating so that the net loading on the system is not affected by it. Two simple methods for generating body loads are now described briefly.

2.2.4 Viscoplastic algorithm

Following viscoplastic algorithm [24], the material is allowed to sustain stresses outside the failure criterion for finite “periods”. Overshoot of the failure criterion as signified by a positive value of the yield criteria F as expressed in eq. (4). Viscoplastic strains are generated at a rate that is related to the amount by which yield has been violated through the expression.

$$\left\{ \overset{\bullet}{\in}^{vp} \right\} = F\left\{ \frac{\partial Q}{\partial \sigma} \right\} \tag{15}$$

Where Q is the plastic potential function.

It should be noted that a pseudo-viscosity property equal to unity is implied on the right hand side of eq. (15) from dimensional considerations. Multiplication of the viscoplastic strain rate by a pseudo-time step gives an increment of viscoplastic strain which is accumulated from one "time-step" or iteration to the next. Thus:

$$\left\{ \delta \in^{vp} \right\}^{i} = \Delta t \left\{ \overset{\bullet}{\in}^{vp} \right\}^{i} \tag{16}$$

and

$$\left\{ \Delta \in^{vp} \right\}^{i} = \left\{ \Delta \in^{vp} \right\}^{i-1} + \left\{ \delta \in^{vp} \right\}^{i} \tag{17}$$

The "time step" for unconditional numerical stability has been derived by Cormeau (1975) and depends on the assumed failure criterion. For Mohr-Coulomb materials:

$$\Delta t = \frac{4(1+\nu)(1-2\nu)}{E\left(1-2\nu+\sin^2\phi\right)} \tag{18}$$

The derivatives of the plastic potential function Q with respect to stresses are conveniently expressed through the Chain Rule, thus:

$$\left\{ \frac{\partial Q}{\partial \sigma} \right\} = \frac{\partial Q}{\partial \sigma_m}\left\{ \frac{\partial \sigma_m}{\partial \sigma} \right\} + \frac{\partial Q}{\partial J_2}\left\{ \frac{\partial J_2}{\partial \sigma} \right\} + \frac{\partial Q}{\partial J_3}\left\{ \frac{\partial J_3}{\partial \sigma} \right\} \tag{19}$$

where J_2 is second invariant of deviatoric stress and the viscoplastic strain rate given by eq. (16) is evaluated numerically by an equation of the form:

$$\left\{ \overset{\bullet}{\in}^{vp} \right\} = F\left(\frac{\partial Q}{\partial \sigma_m}\left[M^1\right] + \frac{\partial Q}{\partial J_2}\left[M^2\right] + \frac{\partial Q}{\partial J_3}\left[M^3\right] \right)\{\sigma\} \tag{20}$$

In the above equation, $\left\{ \frac{\partial \sigma_m}{\partial Q} \right\}$, $\left\{ \frac{\partial J_2}{\partial Q} \right\}$ and $\left\{ \frac{\partial J_3}{\partial Q} \right\}$ are represented by the matrix vector products $\left[M^1\right]\{\sigma\}$, $\left[M^2\right]\{\sigma\}$ and $\left[M^3\right]\{\sigma\}$. This is essentially the notation used by Zienkiewicz and Taylor (1989). The body loads $\{F_b\}^i$ are accumulated at each "time-step" within each load step by summing the following integrals for all elements containing a yielding $(F > 0)$ Gauss point:

$$\{F_b\}^i = \{F_b\}^{i-1} + \sum_{elements}^{all} \iint [B]^T [D^e] \{\Delta \in^{vp}\}^i dxdy \tag{21}$$

This process is repeated at each "time step" iteration until no integrating point stresses violate the failure criterion within the tolerance. The convergence criterion is based on a dimensionless measure of the amount by which the displacement increment vector $\{U\}^i$ changes from one iteration to the next.

2.2.5 Gravity loading

The forces generated by the self-weight of the soil are computed by using a standard gravity "turn-on" procedure involving integrals over each element of the form:

$$p^{(e)} = \gamma \int_{V^e} N^T dV^e \tag{22}$$

where N is the matrix of shape of the functions of the element and the superscript e refers to the element number. This integral evaluates the volume of each element, multiplies by the total unit weight of the soil and distributes the net vertical force consistently to all the nodes. These element forces are assembled into a global gravity force vector that is applied to the finite element mesh in order to generate the initial stress state of the problem.

2.2.6 Influence of free surface and reservoir loading on slope stability

We now consider the influence of a free-surface within an earth slope and reservoir loading on the outside of a slope as shown in Fig. 3.

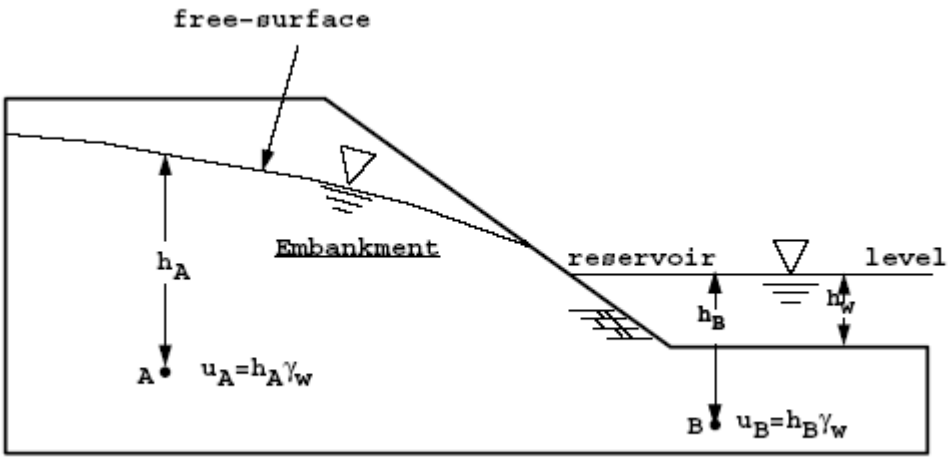

Figure 3. Slope with free-surface and reservoir loading

Regarding the role of the free-surface, a rigorous approach would firstly involve obtaining a good quality flow net for free-surface flow through the slope, enabling pore pressures to be accurately estimated at any point within the flow region. For the purposes of

slope stability analysis however, it is usually considered sufficiently accurate and conservative to estimate pore pressure at a point as the product of the unit weight of water (γ_w) and the vertical distance of the point beneath the free surface. In Fig. 3-9, the pore pressures at two locations, A and B, have been calculated using this assumption.

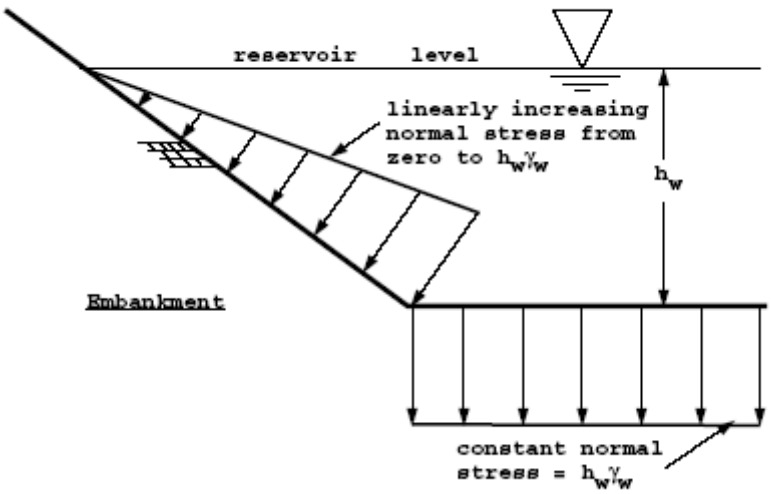

Figure 4. Detail of submerged area of slope beneath free-standing reservoir water showing stresses to be applied to the surface of the mesh as equivalent nodal loads

In the context of finite element analysis, the pore pressures are computed at all submerged (Gauss) points as described above, and subtracted from the total normal stresses computed at the same locations following the application of surface and gravity loads. The resulting effective stresses are then used in the remaining parts of the algorithm relating to the assessment of Mohr-Coulomb yield and elasto-plastic stress redistribution. Note that the gravity loads are computed using total unit weights of the soil. The external loading due to the reservoir is modelled by applying a normal stress to the face of the slope equal to the water pressure. Thus, as shown in Fig. 4, the applied stress increases linearly with water depth and remains constant along the horizontal foundation level. These stresses are converted into equivalent nodal loads in finite element mesh and added to initial gravity loading.

3. NUMERICAL RESULTS

In this section, three example problems are computed to establish the effectiveness of the finite element method is solving slope stability problems. The first problem is simple single layered slope where both the material properties i.e. c (cohesion) and ϕ (angle of internal friction) are considered. The second problem refers to a slope having multi layers. In this case also both c and ϕ are considered as material properties. In the third problem, the effect

of rapid draw down is considered for a homogenous single layered slope. In all the three cases, limit equilibrium methods (i.e. Ordinary slice method, Bishop's method, Spencer's method and Morgenstern and Price's method) are also used to compute the factor of safety and the results are compared to that obtained from FEM. It is observed that the FOS values from limit equilibrium techniques and FEM tallies very well. However, FEM solutions also provide additional data regarding displacements of various points in the soil mass as well as its stress-strain behaviour.

3.1 Problem 1 - A single layered slope

The problem considers a single layered homogeneous, $c' - \phi'$ slope with foundation. The geometry of the slope, finite mesh input, deformed mesh at failure, displacement vectors at failure diagrams are shown in Fig. 5, Fig. 6, Fig. 7 and Fig. 8 respectively. The material parameters for this particular slope are as follows:

$\phi = 10^\circ$, $c' = 9.8$ kPa, $\psi = 0$, $\gamma = 27.64$ kN/m^3, $E' = 1.e5$ kN/m^2 and $\nu' = 0.3$.

Gravity load is applied to the model and the strength reduction factor (SRF) gradually increased affecting eq. 2 and eq. 3 until convergence could not be achieved. The programs used in this paper are based on closely on Program 6.3 in the text by Smith and Griffiths (2004). The programs are for 2-d plane strain analysis of elastic-perfectly plastic soils with Mohr-Coulomb failure criterion utilizing 8-node quadrilateral elements with reduced integration (4 Gauss-points per element) in the gravity loads generation, the stiffness matrix generation and the stress redistribution phases of the algorithm.

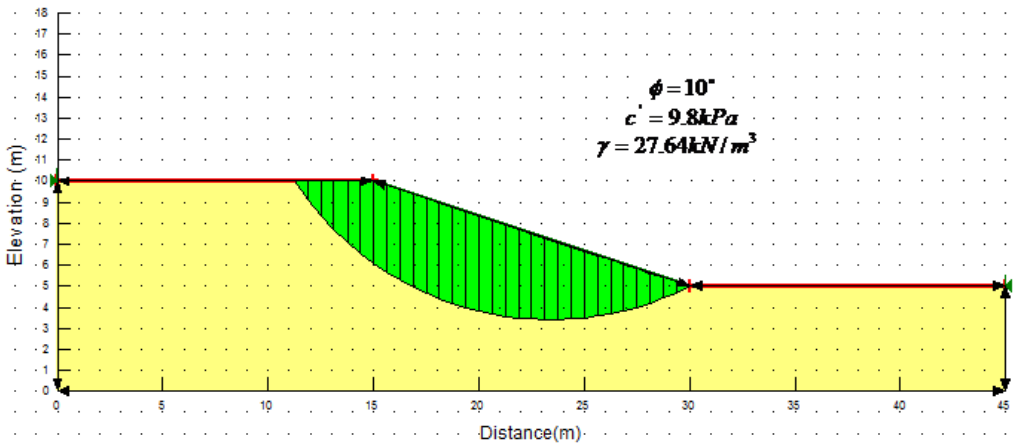

Figure 5. Geometry and material properties of slope in problem 1

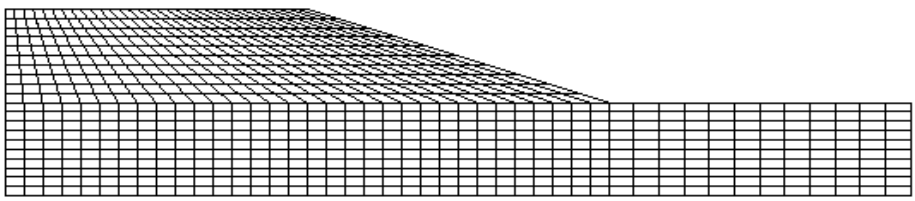

Figure 6. Finite element mesh for the slope in problem 1

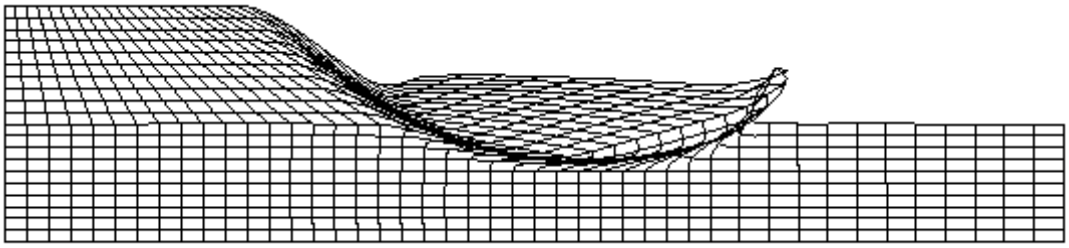

Figure 7. Deformed mesh at failure for problem 1

Figure 8. Displacement vectors at failure for problem 1

The output result for problem 1 from finite element program is shown in Table 1. The Table indicates that five trial strength reduction factors were attempted ranging from 0.5 to 1.2969. Each value represented a completely independent analysis in which the soil strength parameters were scaled by SRF as indicated in eq. (2) and (3). It is possible that the gravity loads and global stiffness matrix are the same in each analysis and are therefore generated once only. The "iterations" column indicates the number of iterations for convergence corresponding to each SRF value. The algorithm has to work harder to achieve convergence as the "true" FOS is approached. When SRF=FOS=1.2969 $\cong$ 1.30, there is a sudden increase in the dimensionless displacement ($E^{'}\delta_{\max} / \gamma H^2$), and the algorithm is unable to converge within the iteration limit of 1000. The obtained factor of safety value from this method is very close to the values obtained from those traditional limit equilibrium methods. Fig. 9 shows a graph of data from Table 1.

Table 1: Finite element method results for problem 1

Trial Factor	Max Displacement	Iterations
0.5000	0.1040e-01	2
1.0000	0.1449e-01	12
1.2500	0.1722e-01	76
1.2812	0.1821e-01	228
1.2969	0.2513e-01	1000

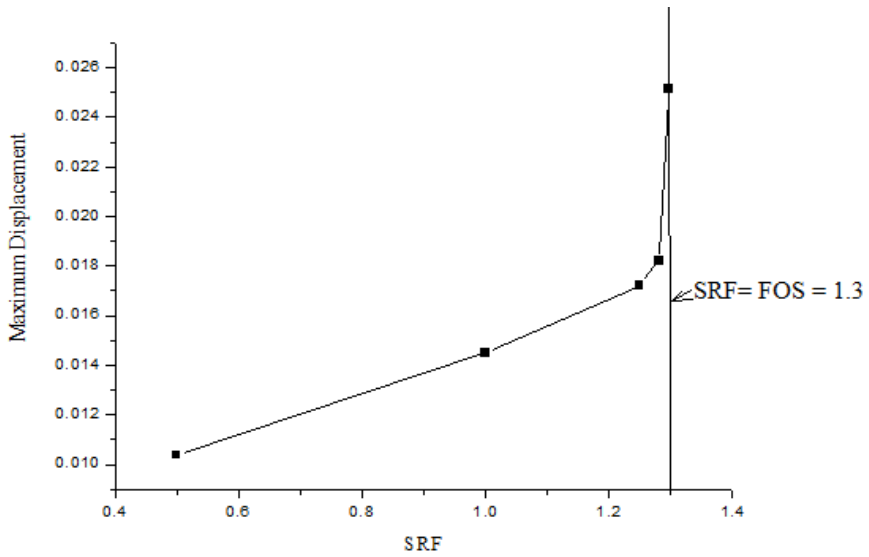

Figure 9. Maximum displacement vs. srf for problem 1

Using SLOPE/W software, the value of factor of safety calculated from traditional limit equilibrium methods for problem 1. Factor of safeties from different methods of problem 1 are listed in Table 2.

Table 2: Factor of safeties from FEM and limit equilibrium methods for problem 1

	Methods				
	Ordinary Slice Method	Bishop's Method	Spencer's Method	Morgenstern and Price Method	Finite Element Method
Factor of safety	1.237	1.316	1.315	1.315	1.3

3.2 Problem 2 - two layered slope

Stability analysis of a two-layer $c' - \phi'$ Slope is carried out in this section. The geometry of the slope, finite mesh input, deformed mesh at failure, displacement vectors at failure diagrams are shown in Fig.10, Fig.11, Fig.12 and Fig.13 respectively. The material parameters for this particular slope are: (1) For layer 1: $\phi = 25^\circ$, $c' = 1$ kPa, $\psi = 0$, $\gamma = 20$ kN/m^3, $E' = 1.e5$ kN/m^2 and $\nu' = 0.3$; (2) For layer 2: $\phi = 15^\circ$, $c' = 0.5$ kPa, $\psi = 0$, $\gamma = 20$ kN/m^3, $E' = 1.e5$ kN/m^2 and $\nu' = 0.3$. The Problem has been solved using program of Smith and Griffiths [19].

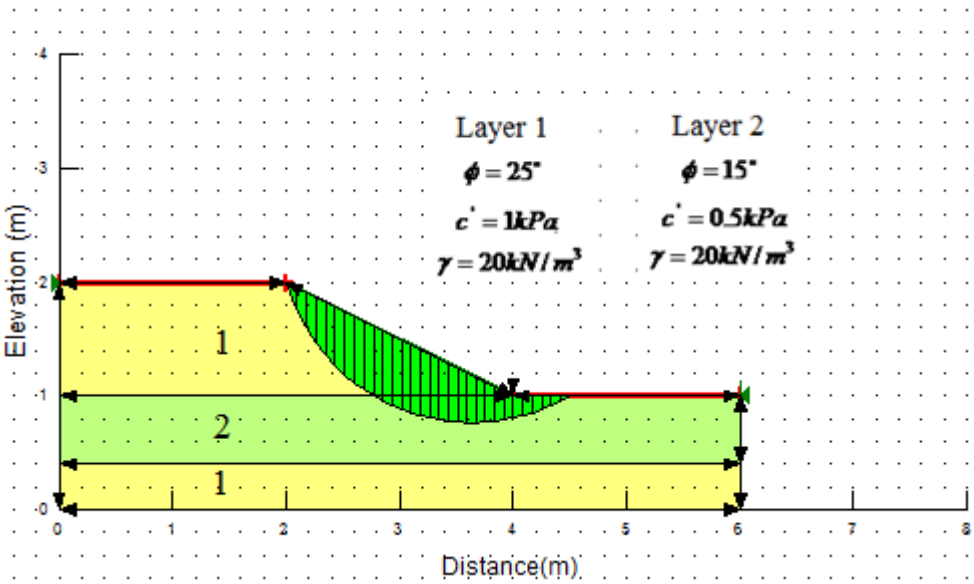

Figure 10. Cross section of slope problem 2

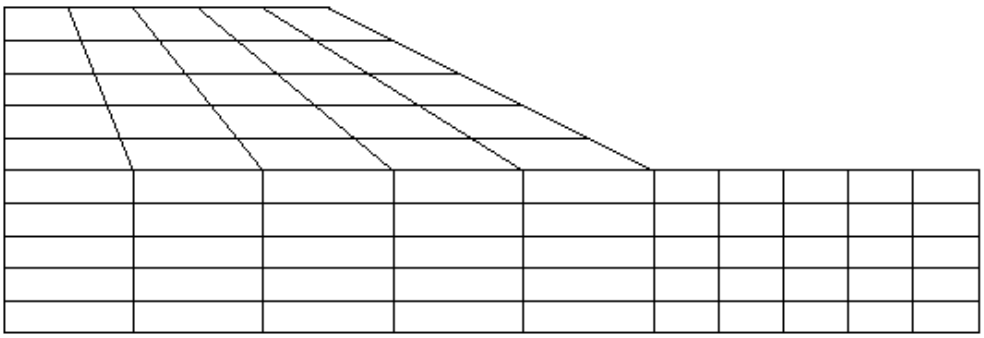

Figure 11. Finite element mesh for problem 2

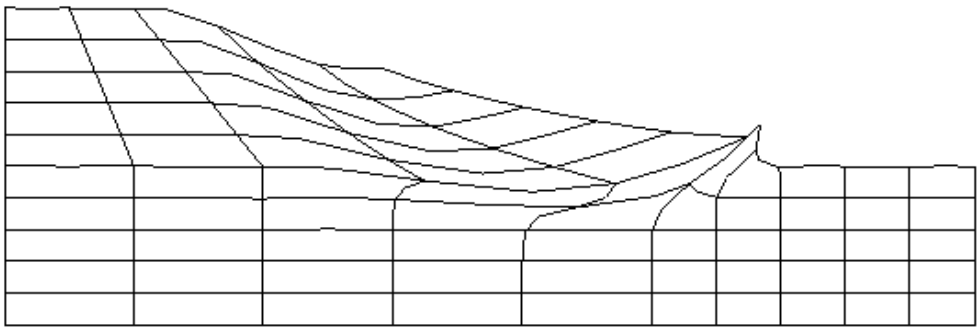

Figure 12. Deformed mesh at failure for problem 2

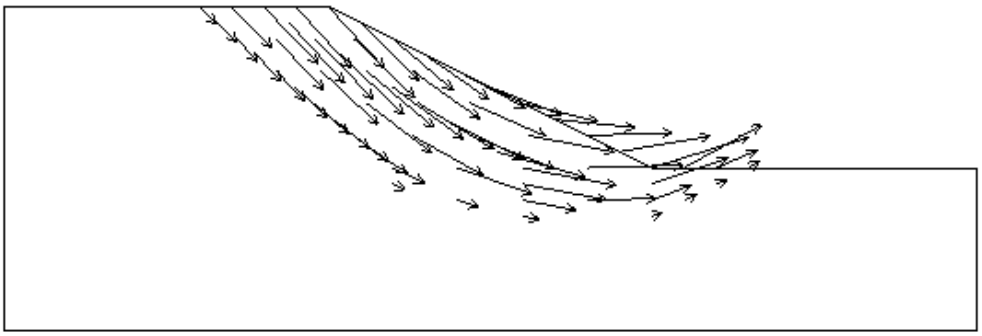

Figure 13. Displacement vectors at failure for problem 2

The output result for problem 2 from finite element program is shown in Table 3. The Table indicates that six trial strength reduction factors were attempted ranging from 0.5 to 1.2344. Each value represented a completely independent analysis in which the soil strength parameters were scaled by SRF as indicated in eqn. (2) and (3). It is possible that the gravity loads and global stiffness matrix are the same in each analysis and are therefore generated once only. The "iterations" column indicates the number of iterations for convergence corresponding to each SRF value. The algorithm has to work harder to achieve convergence as the "true" FOS is approached. When SRF=FOS=1.2344 $\cong$ 1.23, there is a sudden increase in the dimensionless displacement ($E^{'}\delta_{\max} / \gamma H^{2}$), and the algorithm is unable to converge within the iteration limit of 500. The obtained factor of safety value from this method is very close to the values obtained from those traditional limit equilibrium methods. Fig. 14 shows a graph of data from Table 3.

Table 3: Finite element method results for problem 2

Trial Factor	Max Displacement	Iterations
0.5000	0.3043e-03	2
1.0000	0.3383e-03	29
1.1250	0.3600e-03	48
1.1875	0.3824e-03	143
1.2188	0.4241e-03	381
1.2344	0.4857e-03	500

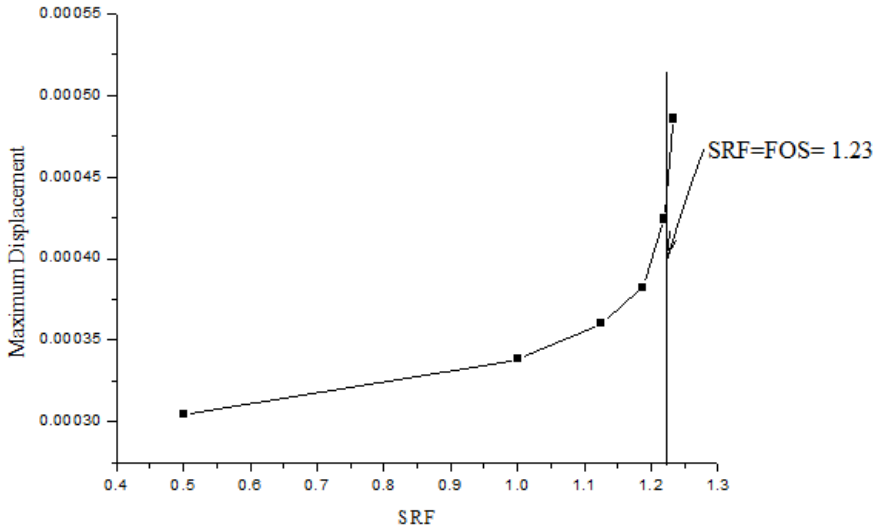

Figure 14. Maximum displacement vs srf for problem 2

Similarly, like problem 1, using SLOPE/W software, the value of factor of safety calculated from traditional limit equilibrium methods for Problem 2. Factor of safeties from different methods of Problem 2 are listed in Table 4.

Table 4: Factor of safeties of problem 2

	Methods				
	Ordinary Slice Method	Bishop's Method	Spencer's Method	Morgenstern and Price Method	Finite Element Method
Factor of safety	1.128	1.293	1.275	1.275	1.23

3.3 Problem 3 (A homogeneous slope including a free surface)

In this section, the stability analysis of a single layered homogeneous, $c' - \phi'$ slope including a free surface is carried out. The geometry of the slope, finite mesh input, deformed mesh at failure, displacement vectors at failure diagrams are shown in Fig.15, Fig.16, Fig.17 and Fig.18 respectively. The material parameters for this particular slope are: $\phi = 5^\circ$, $c' = 200$ kPa, $\psi = 0$, $\gamma = 120$ kN/m^3, $E' = 1.e5$ kN/m^2 and $\nu' = 0.3$. The problem has been solved using the software provided in 4th edition of the book by Smith and Griffiths [19].

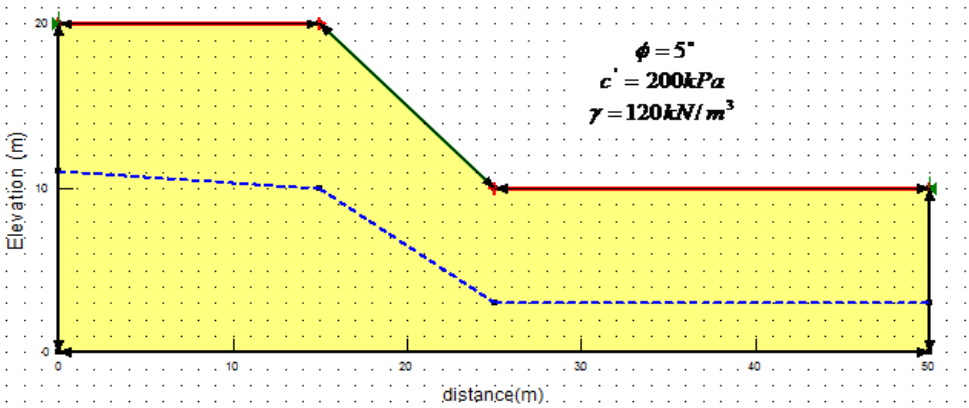

Figure 15. Cross Section of Slope Problem 3

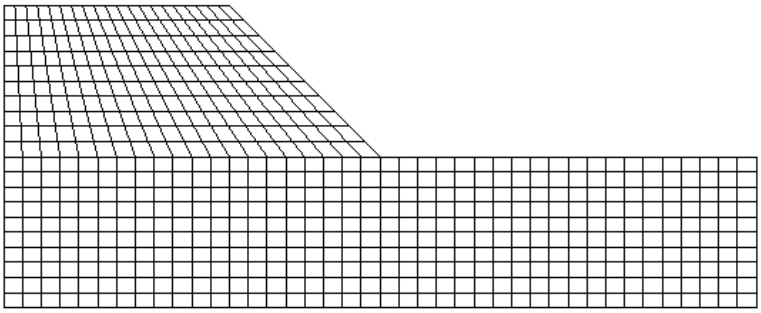

Figure 16. Finite Element Mesh for Problem 3

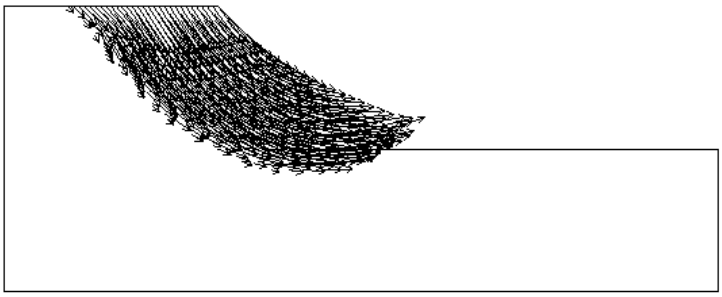

Figure 17. Displacement Vectors at Failure for Problem 3

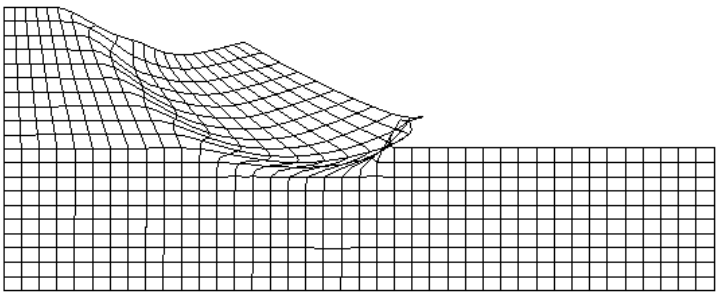

Figure 18. Deformed Mesh at Failure for Problem 3

The output result for problem 3 from finite element program is shown in TABLE 5. The Table indicates that six trial strength reduction factors were attempted ranging from 0.5 to 1.1875. Each value represented a completely independent analysis in which the soil strength parameters were scaled by SRF as indicated in eqn. (2) and (3). It is possible that the gravity loads and global stiffness matrix are the same in each analysis and are therefore generated once only. The "iterations" column indicates the number of iterations for convergence corresponding to each SRF value. The algorithm has to work harder to achieve convergence as the "true" FOS is approached. When SRF=FOS=1.1875 $\cong$ 1.19, there is a sudden increase in the dimensionless displacement ($E^{'}\delta_{\max} / \gamma H^2$), and the algorithm is unable to converge within the iteration limit of 1000. The obtained factor of safety value from this method is very close to the values obtained from those traditional limit equilibrium methods.

Figure 19 shows a graph of data from TABLE 5. The graph of Figure 18, the displaced mesh plot of Figure 17 and vector plot of Figure 16 indicate both the factor of safety and the nature of failure mechanism for problem 3.

Table 5: Finite element method results for problem 3

Trial Factor	Max Displacement	Iterations
0.5000	0.1918e+00	5
1.0000	0.3178e+00	57
1.1250	0.3693e+00	78
1.1562	0.3853e+00	118
1.1719	0.3942e+00	647
1.1875	0.6303e+00	1000

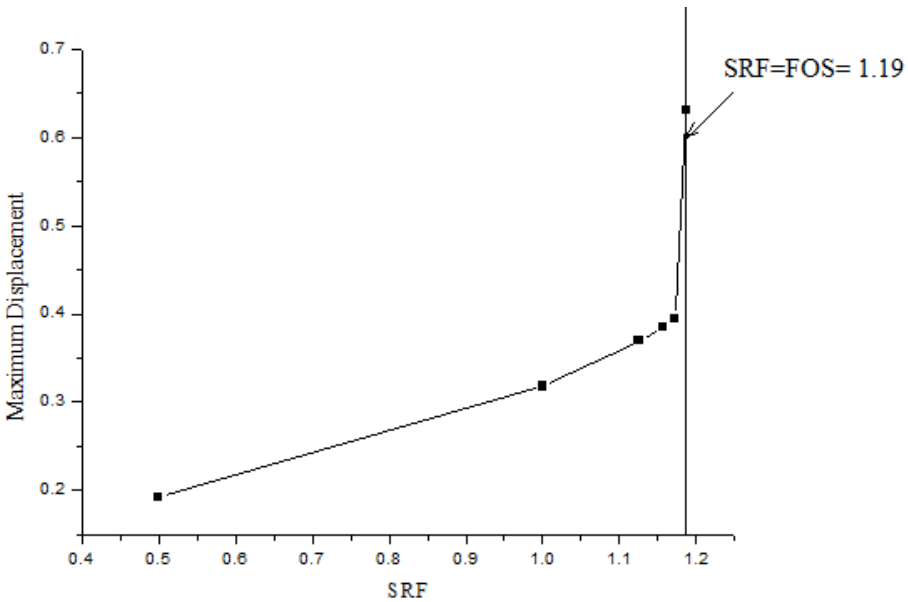

Figure 19. Maximum Displacement Vs Displacement

Table 6: Factor of safeties of problem 3

	Methods				
	Ordinary Slice Method	Bishop's Method	Spencer's Method	Morgenstern and Price Method	Finite Element Method
Factor of safety	1.172	1.182	1.202	1.181	1.19

3.4 Problem 4 - rapid drawdown analysis of a homogenous slope

In this section, the rapid drawdown analysis of a homogenous slope is carried out. The problem has been taken from slope-stab folder of software 4th ed of Smith and Griffiths (2004). The geometry of the slope, finite mesh input, deformed mesh at failure, displacement vectors at failure diagrams are shown in Fig. 20, Fig. 21, Fig. 22 and Fig. 23 respectively. The material parameters for this particular slope are: $\phi = 37^\circ$, $c' = 13.8$ kPa, $\psi = 0$, $\gamma = 18.2$ kN/m^3, $E' = 1.e5$ kN/m^2 and $\nu' = 0.3$.

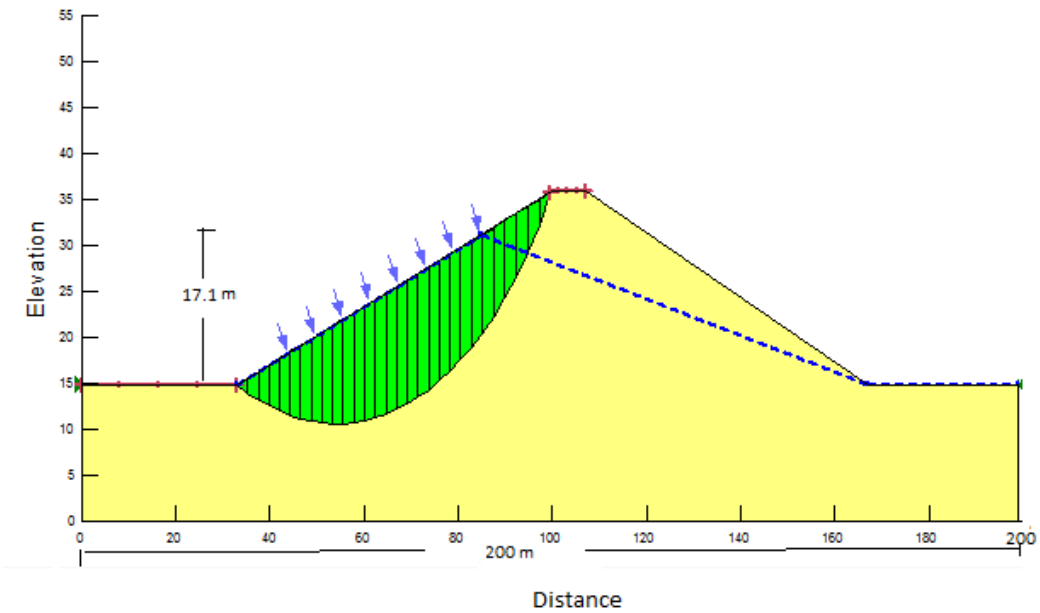

Figure 20. Cross section of slope problem 3

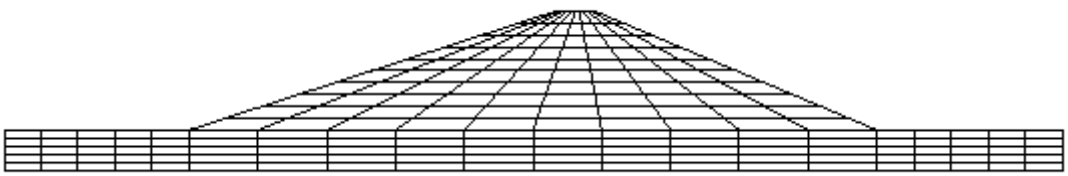

Figure 21. Finite element mesh for problem 3

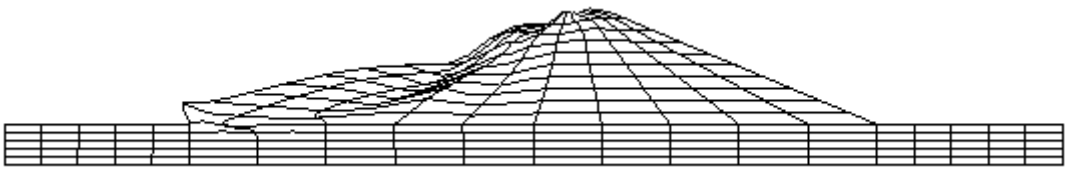

Figure 22. Deformed mesh at failure for problem 3

Figure 23. Displacement vectors at failure for problem 4

The output result for Problem 3 from finite element program is shown in Table 7. The table indicates that six trial strength reduction factors were attempted ranging from 0.5 to 1.5469. Each value represented a completely independent analysis in which the soil strength parameters were scaled by SRF as indicated in eqn. (2) and (3). It is possible that the gravity loads and global stiffness matrix are the same in each analysis and are therefore generated once only. The "iterations" column indicates the number of iterations for convergence corresponding to each SRF value. The algorithm has to work harder to achieve convergence as the "true" FOS is approached. When SRF=FOS=1.5469 $\cong$ 1.55, there is a sudden increase in the dimensionless displacement ($E'\delta_{max}/\gamma H^2$), and the algorithm is unable to converge within the iteration limit of 500. The obtained factor of safety value from this method is very close to the values obtained from those traditional limit equilibrium methods. Fig. 24 shows a graph of data from Table 7.

Table 7: Finite element method results for problem 3

Trial Factor	Max Displacement	Iterations
0.5000	0.5725E-01	41
1.0000	0.6759E-01	38
1.5000	0.9068E-01	113
1.5312	0.9522E-01	269
1.5469	0.9871E-01	500

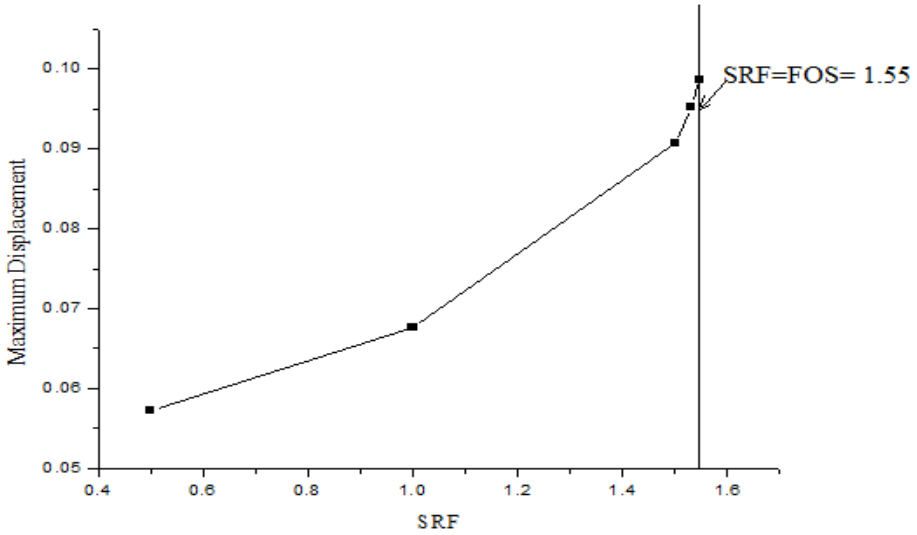

Figure 24. Maximum displacement vs srf for Problem 3

Using SLOPE/W software, the value of factor of safety calculated from traditional limit equilibrium methods for problem 3. For this particular problem, analysis is done for a) with rapid draw down case and b) without rapid draw down case. Factor of safeties from different methods of problem 3 are listed in Table 6.

Table 8: Factor of safeties of problem 3

Problems		Methods				
		Ordinary Slice Method	Bishop's Method	Spencer's Method	Morgenstern and Price Method	Finite Element Method
Problem 3	With rapid draw down	1.597	1.956	1.961	1.960	1.55
	Without rapid draw down	2.365	2.519	2.517	2.517	2.42

The factor of safeties calculated using different limit equilibrium methods and finite element method are listed together in Table 7. For the rapid draw down case, it is observed that the calculated value of FOS is lowest which is not applicable for the other cases. For rapid draw down case, the pore pressures are computed for all the gauss points for the submerged elements and are subtracted from the normal stresses. The authors conclude that there is a overestimation of the subtracted pore water pressure because it is done for all the four Gauss points of the elements which are submerged. In case of limit equilibrium techniques, pore pressures are only subtracted for the portion of slices which are submerged. Because while estimating the FOS using FEM, the subtraction is carried out for all the single submerged elements, the overall subtracted value of pore water pressure is greater than that subtracted while using limit equilibrium techniques. This phenomenon leads to lower

estimation albeit more conservative estimation of FOS when the effect of rapid draw down is considered.

Table 7: Summary of the results of all problems

Problems		Methods				
		Ordinary Slice Method	Bishop's Method	Spencer's Method	Morgenstern and Price Method	Finite Element Method
Problem 1		1.237	1.316	1.315	1.315	1.3
Problem 2		1.128	1.293	1.275	1.275	1.23
Problem 3		1.172	1.182	1.202	1.181	1.19
Problem 4	With rapid draw down	1.597	1.956	1.961	1.960	1.55
	Without rapid draw down	2.365	2.519	2.517	2.517	2.42

4. CONCLUSION

In the present work, limit equilibrium technique (ordinary slice method, Bishop's method, Spencer's method, Morgenstern-Price method) and finite element method have been used to the study different slope stability problems. Also, it is observed that ordinary slice method provides most conservative estimation of factor of safety values amongst all the limit equilibrium techniques considered in this paper. Therefore, any design of slopes carried out with ordinary slice method is likely to be always on the safer side. Other limit equilibrium methods like Ordinary Bishop's Method, Spencer's Method and Morgenstern and Price's method attempt to establish a more realistic estimation of interslice forces which may develop in reality. But they lead to somewhat higher estimation of factor of safety. The FOS values obtained using finite element method compare very well with that obtained from limit equilibrium methods. In finite element method, the FOS for critical slip surface is automatically obtained. In case of limit equilibrium methods, several slip surfaces should be analysed to find the critical slip surface. These types of trial and error calculations are not required with FEM to find out the critical slip surface because the failure occurs through the zone of weakest material properties and automatically the critical slip surface is determined. Furthermore, finite element method satisfies the equations of equilibrium and compatibility equations from theory of elasticity. Therefore, it serves as a more mathematically robust platform. Also, displacements, stress and strains at various nodes in the slope domain are also obtainable from finite element method. These are few of the additional benefits of using finite element method.

REFERENCES

1. Schuster RL. Socioeconomic significance of landslides: investigation and mitigation,

Transportation Research Board, Washington special report 247, (1996) 12-35.

2. Hutchinson JN. Keynote paper: Landslide hazard assessment, *Proceedings of the 6th International Symposium Landslides*, Christchurch, Balkema, Rotterdam, **3**(1995) 1805-41.
3. Li T. Landslides - extent and economic significance in China, Brabb EE, Harrod BL. Eds, Landslides - extent and economic significance: Rotterdam, Netherlands, AA Balkema Publishers, (1989) 271-87.
4. Fellenius W. Calculation of stability of earth dams, *Proceedings of the 2nd Congress on Large Dams*, U.S. Government Printing Office, Washington D.C, **4**(1936).
5. Bishop AW. The use of slip circle in the stability analysis of slopes, *Geotechnique*, No. 1, **5**(1955) 7-17.
6. Spencer E. A method of analysis of the stability of embankments assuming parallel inter-slice forces, *Geotechnique*, No. 1, **17**(1967) 11-26.
7. Janbu N. Stability analysis of slopes with dimensionless parameters, *Harvard Soil Mechanics Series*, **46**(1954) 81 p.
8. Morgenstern NR, Price VE. The analysis of the stability of general slip surfaces, *Geotechnique*, No. 1, **15**(1965) 79-93.
9. Duncan JM. State of the art: Limit equilibrium and finite-element analysis of slopes, *Journal of Geotechnical Engineering, ASCE*, No. 7, **122**(1996) 577-96.
10. Griffiths DV, Lane PA. Slope Stability analysis by finite elements, *Geotechnique*, No. 3, **49**(1999) 387-403.
11. Smith IM, Hobbs R. Finite element analysis of centrifuged and built-up slopes, *Geotechnique*, No. 4, **24**(1974) 531-59.
12. Taylor DW. Stability of earth slopes, *Journal of the Boston Society of Civil Engineers*, **24**(1937) 197-246.
13. Zienkiewicz OC, Humpheson C, Lewis RW. Associated and non-associated viscoplasticity and plasticity in soil mechanics, *Geotechnique*, **25**(1975) 671-89.
14. Griffiths DV. Finite element analysis of walls, footings and slopes, PhD Thesis, Department of Engineering, University of Manchester, 1980.
15. Potts DM, Dounias GT, Vaughan PR. Finite element analysis of progressive failure of Carsington Embankment, *Geotechnique*, No. 1, **40**(1990) 79-102.
16. Lane PA, Griffiths DV. Assessment of stability of slopes under drawdown conditions, *Journal of Geotechnical and Geoenvironmental Engineering, ASCE*, No. 5, **126**(2000) 443-50.
17. Li X. Finite element analysis of slope stability using a nonlinear failure criterion, *Computers and Geotechnics*, **34**(2007) 188-95.
18. Smith IM, Griffiths DV. *Programming the Finite Element Method*, 3rd edition, John Wiley and Sons, Chichester, New York, 1998.
19. Smith IM, Griffiths DV. *Programming the Finite Element Method*, 4th edition, John Wiley and Sons, Chichester, New York, 2004.
20. Lehman JB, Griffiths DV. Analysis of the progression failure in earth slopes by finite elements, *Slope Stability 2000, Proceedings of the GeoDenver Symposium*, Geotechnical Special Publication, ASCE, No. 101, (2000), pp. 250-265.
21. Griffiths DV, Marquez RM. Three-dimensional slope stability analysis by Finite elements, *Geotechnique*, No. 6, **57**(2007) 537-46.

22. Dawson EM, Roth WH, Drescher A. Slope Stability Analysis by Strength, *Geotechnique*, No. 6, **49**(1999) 835-40.
23. Matsui T, Sun KC. Finite element slope stability analysis by shear strength reduction technique, *Soils and Foundations,* No. 1, **32**(1992) 59-70.
24. Zienkiewicz OC, Cormeau IC. Viscoplasticity, plasticity and creep in elastic solids. A unified numerical solutions approach, *International Journal of Numerical Methods in Engineering*, **8**(1974) 821-45.